https://doi.org/10.46813/2024-152-064

UDC 621.039.53

SYNTHESIS OF MATERIALS BASED ON COMPOUNDS OF RARE EARTH ELEMENTS WITH TITANIUM, HAFNIUM AND ZIRCONIUM AS PROMISING NEUTRON ABSORBERS FOR NUCLEAR REACTORS

I.O. Chernov[1], A.V. Kushtym[1], S.V. Malykhin[2]

[1] National Science Center "Kharkov Institute of Physics and Technology" "Nuclear Fuel Cycle" Science and Technology Establishment, Kharkiv, Ukraine;

[2]National Technical University "Kharkiv Polytechnic Institute", Kharkiv, Ukraine

E-mail: chernov@kipt.kharkov.ua

A review of the methods for the synthesis of titanates, hafnates, and zirconates of rare earth elements, primarily dysprosium, which have been applied as neutron-absorbing materials for nuclear reactors or are promising due to their high radiation resistance, phase stability, compatibility with structural materials, and corrosion resistance is presented. The characteristics of titanates, hafnates, and zirconates of dysprosium obtained by these methods are presented: high-temperature solid-phase synthesis in compacted mixtures of initial oxides; induction melting of oxides in a "cold" container; chemical methods based on co-precipitation and heat treatment of aqueous solutions; mechanochemical activation of oxide powders in planetary mills followed by heat treatment; plasma-chemical synthesis.

INTRODUCTION

Neutron-absorbing materials are an integral component of the rod cluster control assembly (RCCA) control rods (CRs) of nuclear reactors. The function of the RCCAs is to provide for the rapid termination of a nuclear reaction, maintain reactor power at a given level and transfer it from one level to another.

In the current design of WWER-1000 CRs, dysprosium titanate ($Dy_2O_3 \cdot TiO_2$) and boron carbide (B_4C) are applied as neutron-absorbing materials in the form of powder fills in the cladding [2]. It is also relevant to develop new and promising neutron-absorbing materials with increased performance, one of which is dysprosium hafnate ($HfO_2 \cdot Dy_2O_3$), characterized by high radiation resistance and physical efficiency of neutron absorption under long-term operation [3, 4]. The pellet version of the neutron absorber is considered promising due to the higher density of the CR absorbing stack [5, 6]. Varying the combination of elements (oxides) and providing a certain ratio of them in the composition, as well as the density of materials, causes quite different physical efficiency of neutron absorption.

The Central Research Institute of Electric Power Industry (CRIEPI, Japan) and AREVA NP (France) introduced a new concept of accident-tolerant control rod (ATCR) to improve the safety of light water reactors PWRs and BWRs under all conditions, including severe accidents [1]. This concept is based on the application of alternative neutron-absorbing materials with the following properties: high neutron absorption efficiency, higher melting point and eutectic temperature of more than 1200 °C. Fig. 1 shows that the materials with a physical neutron absorption efficiency similar to B_4C are europium zirconate and hafnate (Eu_2ZrO_5 and Eu_2HfO_5). Materials analogous to the Ag-In-Cd alloy in terms of physical efficiency are: Dy_2ZrO_5, Dy_2HfO_5, Dy_2SmO_5, $Eu_2Zr_7O_7$, HfC.

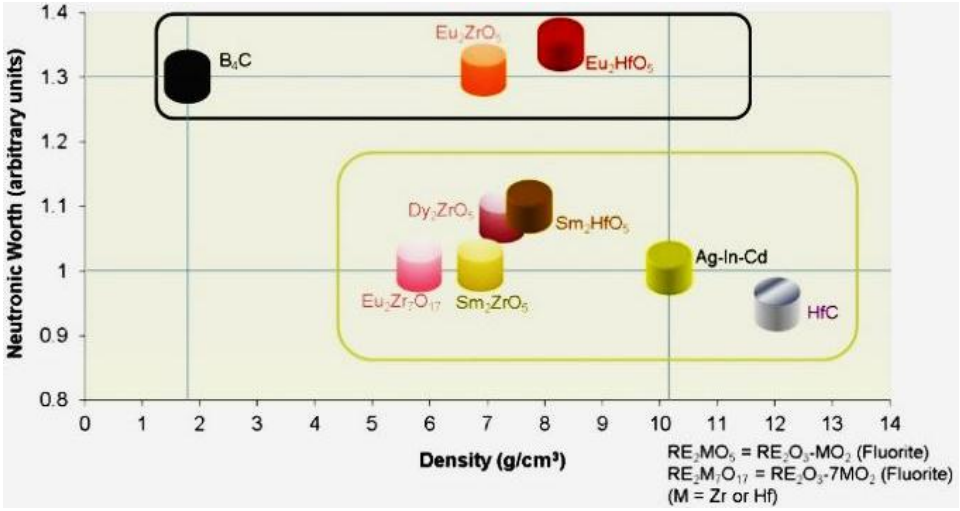

Fig. 1. Density and relative physical efficiency of promising absorbing materials [1]

It is proposed to partially replace dysprosium oxide in the initial fusion mixture with chemically similar oxides to expand the range of dysprosium hafnate ($Dy_2O_3 \cdot HfO_2$) control of the initial physical efficiency. Thus, the application of gadolinium oxide (Gd_2O_3) in the amount of 5% was proposed [7]. In the combination of dysprosium hafnate with gadolinium $n(Dy,Gd)_2O_3 \cdot mHfO_2$, three control rods are applied, each of them absorbs neutrons of different energies efficiently. The thermal neutron absorption cross section of gadolinium is 46000 barn, while that of boron-10 is 3840, dysprosium is 950, and hafnium is 105 barn.

The analysis of phase diagrams of titanium, hafnium, or zirconium oxide binary systems with dysprosium oxide revealed the possibility of obtaining titanates, hafnates, and dysprosium zirconates with single-phase structures [8–12].

The analysis of technological solutions for the synthesis of neutron-absorbing materials based on compounds of rare earth elements with titanium, hafnium, and zirconium, as well as the study of their compositions and pellet characteristics, is of current interest.

STRUCTURAL DIAGRAMS OF $Dy_2O_3 \cdot MeO_2$ SYSTEMS, WHERE Me = {Ti, Hf, Zr}

Dysprosium titanate has the chemical formula Dy_2TiO_5 and can exist in three polymorphic modifications depending on the synthesis temperature [8, 9]. The low-temperature modification of dysprosium titanate is rhombic (α-modification), which at 1350 °C transforms into a hexagonal β-modification, which at 1680 °C transforms into a fluorite structure (F) that melts at 1870 °C (Fig. 2).

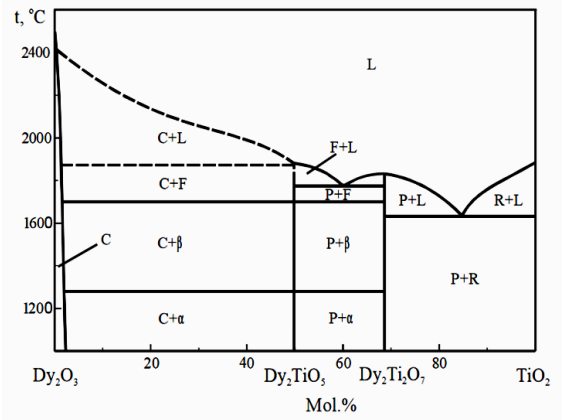

Fig. 2. Structural diagram of the Dy_2O_3-TiO_2 system: α – rhombic phase; β – hexagonal phase; F – fluorite; P – pyrochlore; L – liquid; C – cubic Dy_2O_3; R – rutile TiO_2

Dysprosium dititanate ($Dy_2Ti_2O_7$) crystallizes at a temperature of 770 °C into a pyrochlore crystal structure and melts at a temperature of 1850 °C. $Dy_2Ti_2O_7$ has a cubic face-centered lattice (space group *Fd3m*) with a parameter a = 10.132 Å. The pyrochlore structure is derived from the fluorite structure.

According to the diagram of the Dy_2O_3-HfO_2 system, solid solutions with a single-phase structure such as fluorite, for which there is no phase transition in the entire temperature range (up to the melting point), exist in the range of solutions with a Dy_2O_3 content of approximately 10...58% (Fig. 3) [10, 11].

The analysis of the Dy_2O_3-ZrO_2 system shows that the areas of a solid solution of the fluorite type at a temperature of 400 °C are from 15 mol.% Dy_2O_3 to 43 mol.% Dy_2O_3 (Fig. 4) [12–14].

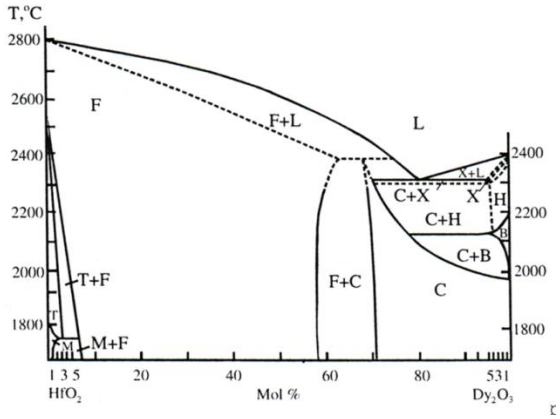

Fig. 3. Structural diagram of the Dy_2O_3-HfO_2 system: F – fluorite; C – solid solution based on Dy_2O_3; M, T – monoclinic and tetragonal modifications of HfO_2; X, H, B – high-temperature polymorphic modifications of Dy_2O_3 [10]

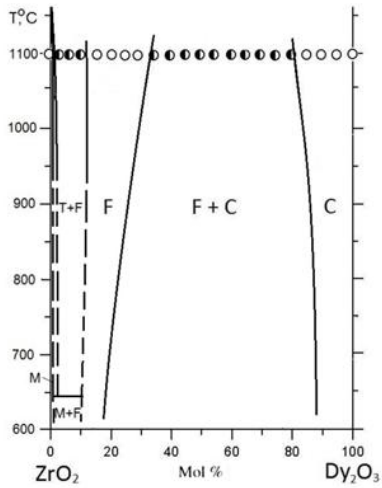

Fig. 4. Phase equilibrium diagram of Dy_2O_3-ZrO_2 systems: Fss (F) – fluorite; Css (C) – solid solution based on Er_2O_3 [14]

SOLID-PHASE SYNTHESIS

DYSPROSIUM TITANATE

The solid-phase synthesis of dysprosium titanate has been studied by many groups of researchers in various scientific centers [13–22]. The solid-phase synthesis is performed by high-temperature heating of mechanical pelletized mixtures of dysprosium and titanium oxides in air [14]. The dysprosium titanate synthesized in this way can contain unreacted residues of the initial oxides and intermediate reaction products [21]. For example, in [15], it was reported that low-temperature sintering, 1300 °C, results in the reaction between precursors and the formation of dysprosium titanate. It is assumed that the formation of Dy_2TiO_5 from precursors is a two-stage process, when dysprosium dititanate ($Dy_2Ti_2O_7$) is formed between 800 and 1050 °C, and dysprosium titanate (Dy_2TiO_5) is formed according to the reaction

$Dy_2Ti_2O_7$ + Dy_2O_3. The authors of this paper managed to obtain three structures of dysprosium titanate (rhombic, hexagonal, cubic) depending on the sintering conditions (temperature, cooling rate) (Fig. 5).

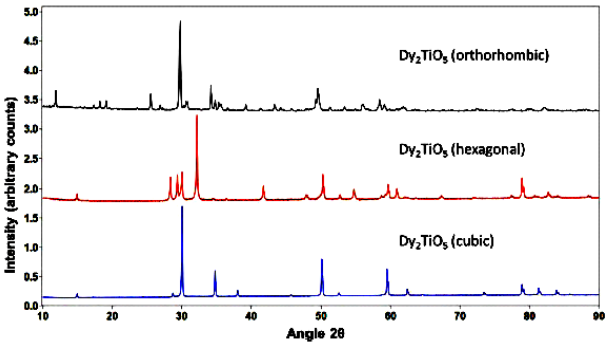

Fig. 5. Powder X-ray diffraction patterns for the three main phases of Dy_2TiO_5: orthorhombic Pnma, hexagonal P63/mmc, and cubic Fd-3m [15]

Sintering at 1630 °C with rapid 30...50 °C/min cooling to a temperature of 1000 °C was performed to obtain Dy_2TiO_5 in a bulk single-phase symmetric structure. This enabled to achieve a sufficient level of symmetry. This cooling rate was sufficient to obtain single-phase Dy_2TiO_5 with hexagonal symmetry.

The formation of a bulk single-phase Dy_2TiO_5 composition with hexagonal symmetry was described by Seymour et al. [19]. In the study by Lau [20], it was shown that solid solutions from Dy_2TiO_5 to $Dy_2Ti_2O_7$, which possess the cubic structure of Fd-3m pyrochlore, can be obtained only at high temperatures, which is achieved by arc melting and rapid cooling.

An alternative method for obtaining Dy_2TiO_5 with cubic symmetry was described by Sinha and Sharma [16], where it was shown that the addition of molybdenum oxide (MoO_3) to dysprosium titanate compositions of 39.05gDy_2O_3-9.85gTiO_2%-1.35gMoO_3 stabilizes the cubic structure of fluorite at temperatures below the equilibrium temperature of 1680 °C.

Table 1 provides a comparison of the phase composition of both MoO_3-doped and unalloyed dysprosium titanate compositions.

Table 1

Research results of dysprosium titanate pellets [16]

Temperature, °C	Doped MoO_3		Non-doped	
	Exposure time, h	Phase composition	Exposure time, h	Phase composition
600	14	Dy_2O_3+TiO_2	–	–
700	3	$Dy_2Ti_2O_7$+Dy_2O_3+TiO_2	–	–
800	9,5	$Dy_2Ti_2O_7$+Dy_2O_3+TiO_2	12	$Dy_2Ti_2O_7$+Dy_2O_3+TiO_2
850	2	$Dy_2Ti_2O_7$+Dy_2O_3+TiO_2	–	–
900	2	$Dy_2Ti_2O_7$+Dy_2O_3+TiO_2	–	–
950	2	$Dy_2Ti_2O_7$+Dy_2O_3	–	–
1050	2	$Dy_2Ti_2O_7$+Dy_2O_3	2	$Dy_2Ti_2O_7$+Dy_2O_3
1100	2	Dy_2TiO_5(orthorhomb.)+$Dy_2Ti_2O_7$ +Dy_2O_3	–	–
1150	2	Dy_2TiO_5(hex.)+$Dy_2Ti_2O_7$+Dy_2O_3	–	–
1250	2	Dy_2TiO_5(cub.)+$Dy_2Ti_2O_7$	2	Dy_2TiO_5(orthorhomb.)+ $Dy_2Ti_2O_7$
1350	2	Dy_2TiO_5(cub.)+$Dy_2Ti_2O_7$	–	–
1450	2	Dy_2TiO_5(cub.)+$Dy_2Ti_2O_7$	2	Dy_2TiO_5(orthorhomb.)+ Dy_2TiO_5 (hex.)
1550	2	Dy_2TiO_5(cub.)+$Dy_2Ti_2O_7$	2	Dy_2TiO_5(hex.)
1650	4	Dy_2TiO_5(cub.)+$Dy_2Ti_2O_7$	2	Dy_2TiO_5(hex.)

The pellets sintered at 1600 °C for 4 h exhibited a density of ~7 g/cm^3 (97.4% of theoretical), characterized by a two-phase structure of Dy_2TiO_5 (cub.) + $Dy_2Ti_2O_7$ and a fine-grained structure with an average grain size of (5±0.9) μm.

This paper also discusses the mechanism of stabilization of a high-temperature cubic structure such as fluorite by the addition of MoO_3. It is assumed that the addition of MoO_3 in the Dy_2TiO_5 lattice results in the replacement of Ti^{+4} ions by Mo^{+6} ions and the formation of positive charges due to the fact that Mo^{+6} has an ionic radius of 0.059 nm, which is very close to the radius of Ti^{+4} (0.061 nm) for coordination number six [16]. To compensate for these charges, two additional point defects are formed, namely dysprosium vacancies with a negative charge, the concentration of which depends on the concentration of molybdenum in the solid solution. The reaction of defect formation is as follows [15]:

$$Dy_2TiO_5 + x.MoO_3 \rightarrow x.Mo_{Ti}^{\bullet\bullet} + 2x/3\,V_{Dy}^{'''} + (1-x)Ti_{Ti}^{x} + 5O_O^x + x/3\,Dy_2TiO_5 + 2x/3\,TiO_2 + (2-2x/3)Dy_{Dy}^{x}$$

The results of the research into the effect of sintering temperature on the structural and phase state of pellets of 50 mol.% TiO_2 + 50 mol.% Dy_2O_3 (composition No. 1) and 56 mol.% TiO_2 + 44 mol.% Dy_2O_3 (composition No. 2) are given in Table 2 [21].

Table 2

Phase composition of dysprosium titanate synthesis products at temperatures in the range of 1250...1650 ºC

Temperature, °C	Phase composition	Concentration, wt.%	Lattice parameter, nm	Concentration, wt.%	Lattice parameter, nm
1250	Dy_2O_3	38.9	a = 1.066	18.2	a = 1.0657
	TiO_2-ru	2.9	a = 0.4588; c = 0.2963	–	–
	$Dy_2Ti_2O_7$-p	32.0	a = 1.0124	43.4	a = 1.0121
	Dy_2TiO_5-o	26.2	a = 1.0368; b = 1.1219; c = 0.3720	38.4	a = 1.0362; b = 1.1221; c = 0.3717
1350	Dy_2O_3	27.4	a = 1.0664	9.8	a = 1.0659
	$Dy_2Ti_2O_7$-p	38.8	a = 1.0128	37.4	a = 1.0124
	Dy_2TiO_5-o	33.8	a = 1.0372; b = 1.1228; c = 0.3721	52.8	a = 1.0365; b = 1.1229; c = 0.3718
1450	Dy_2O_3	9.2	a = 1.0661	–	–
	$Dy_2Ti_2O_7$-p	29.0	a = 1.0131	35.8	a = 1.0143
	Dy_2TiO_5-h	31.9	a = 0.3632; c = 1.1910	51.3	a = 0.3631; c = 1.1876
	Dy_2TiO_5-f	29.9	a = 0.5211	–	–
	Dy_2TiO_5-p	–	–	12.9	a = 1.0418
1550	Dy_2O_3	3.8	a = 1.0661	–	–
	$Dy_2Ti_2O_7$-p	20.9	a = 1.0142	33.7	a = 1.0143
	Dy_2TiO_5-h	42.5	a = 0.3631; c = 1.1894	64.3	a = 0.3631; c = 1.1876
	Dy_2TiO_5-f	32.8	a = 0.5200	–	–
	Dy_2TiO_5-p	–	–	2	a = 1.0410
1650	Dy_2O_3	1.2	a = 1.0669	–	–
	$Dy_2Ti_2O_7$-p	17.3	a = 1.0167	26.8	a = 1.0161
	Dy_2TiO_5-h	44.9	a = 0.3633; c = 1.1891	73.2	a = 0.3630; c = 1.1860
	Dy_2TiO_5-f	36.6	a = 0.5188	–	–

The formation of low-temperature phases of the orthorhombic structure Dy_2TiO_5-o and the pyrochlore-type structure $Dy_2Ti_2O_7$-p was observed in the pellet material of both compositions after sintering at temperatures of 1250...1350 °C. In both cases, dysprosium oxide was observed. An increase in the sintering temperature to 1450 °C results in the formation of the pyrochlore $Dy_2Ti_2O_7$-p, hexagonal Dy_2TiO_5-h, and fluorite Dy_2TiO_5-f structures in the material of composition No. 1. Dy_2O_3 was also observed in the amount of ~ 9 wt.%. In the material of composition No. 2, three phases were observed at a synthesis temperature of 1450 °C. The first of them, which forms the basis of the material, had the hexagonal structure of Dy_2TiO_5-h, and the other two had the pyrochlore structure of $Dy_2Ti_2O_7$-p and Dy_2TiO_5-p. A decrease of the $Dy_2Ti_2O_7$-p phase and an increase in the content of the Dy_2TiO_5-h phase in the pellet material of both compositions was observed with an increase in the sintering temperature to 1650 °C. Dy_2O_3 was observed in the amount of 1.2 wt.%.

The material of dysprosium titanate pellets of composition No. 2 after sintering at 1650 °C was two-phase and included a phase with a hexagonal structure Dy_2TiO_5-h in the amount of 73.2 wt.% and a phase with a pyrochlore structure $Dy_2Ti_2O_7$-p in the amount of 26.8 wt.%. It should be noted that this phase composition is equilibrium for a given powder composition of dysprosium titanate (see Table 2).

Thus, as a result of the performed studies, it was confirmed that at the temperature range of 1250...1650 °C, the synthesis occurs with the formation and decomposition of low-temperature modifications of dysprosium titanate and intermediate structure of dysprosium dititanate according to the following

$$(Dy_2Ti_2O_7): Dy_2O_3+2TiO_2 \rightarrow Dy_2Ti_2O_7, \quad (1)$$

$$Dy_2O_3+Dy_2Ti_2O_7 \rightarrow 2Dy_2TiO_5. \quad (2)$$

Our studies have confirmed that the doping of MoO_3 results in an increase in the density of dysprosium titanate pellets of the composition 81.2 wt.% Dy_2O_3 + 15.8 wt.% TiO_2 + 3.0 wt.% MoO_3 sintered at a temperature of 1650 °C to 7.1 g/cm^3 compared to the undoped composition and the formation of a single-phase structure of pyrochlore Dy_2TiO_5-p [22].

DYSPROSIUM HAFNATE

To study the kinetics of the dysprosium hafnate synthesis processes, compacted samples were annealed at 1200...1500 °C for 0.25...40 h [13]. It was observed that the interaction reaction occurs by unilateral or predominantly unilateral diffusion of one of the components [13]. It was established that the formation of a crystalline product lags behind the binding of oxides into a solid solution (Fig. 6).

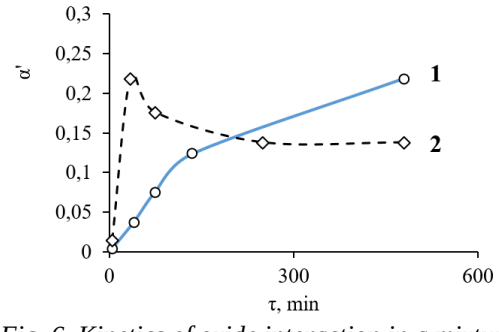

Fig. 6. Kinetics of oxide interaction in a mixture of Dy_2O_3 + HfO_2: 1 – final product; 2 – intermediate product [13]

When HfO_2 interacts with Dy_2O_3, an intermediate solid solution of $Hf_{1-x}Dy_xO_y$ with $x<0.5$ is initially formed, and only as the reaction proceeds, a final solid solution of the composition $Hf_2Dy_2O_7$ with a fluorite-type structure is formed [14]. The analysis of the kinetic curves (see Fig. 6) revealed that the synthesis of dysprosium hafnate is limited by the diffusion of the initial components through the reaction product [23].

It has been shown that the interaction reaction occurs by one-way diffusion or predominantly one-way diffusion of Dy ions into the HfO_2 lattice (Fig. 7) with a diffusion coefficient $D_0 = 1.2 \cdot 10^{-11}$ cm^2/s [24].

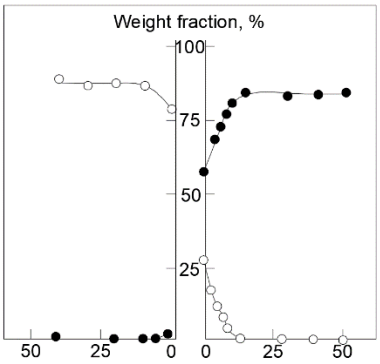

Fig. 7. Distribution of dysprosium (○) and hafnium (●) content in the boundary region after calcination for 3 h at 1800 °C [24]

As the reaction proceeds, a solid solution of dysprosium hafnate is formed with a composition close to the ratio of the initial components [23].

It is well known that the rate of solid-phase reactions depends on the dispersivity and method of obtaining the initial reagents. Such a study was performed in [25]. The starting materials used were HfO_2 obtained by the plasma method with different particle diameters (D); commercial hafnium dioxide (99.9% HfO_2, with a particle size of ≤2000 nm), as well as neodymium, samarium, and dysprosium oxides with a Ln_2O_3 content of at least 99.5% and a particle size of ≤2000 nm.

The X-ray diffraction patterns obtained during the heating process show that hafnium dioxide (D = 50...138 nm) begins to react with Ln_2O_3 at 1100 °C. The beginning of the hafnium dioxide (D = 1000...2000 nm) interaction with Nd_2O_3 and Sm_2O_3 is observed only at 1200 °C, and with Dy_2O_3 – even at 1300 °C. The results of high-temperature X-ray diffraction of mixtures of $Nd_2O_3 + 2HfO_2$, $Sm_2O_3 + 2HfO_2$, $Dy_2O_3 + 2HfO_2$ at different dispersivities are given in Fig. 8.

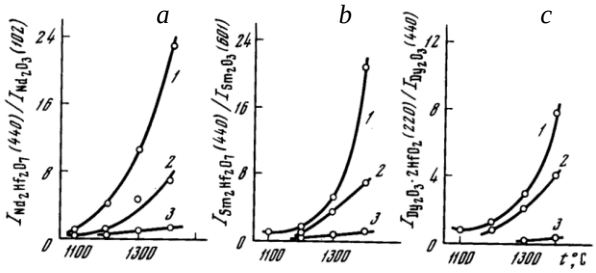

Fig. 8. The ratio of the reaction product reflex intensities to the Ln_2O_3 reflex intensities depending on the temperature and particle size (D) of HfO_2 in the mixtures: $Nd_2O_3 + HfO_2$ (a), $Sm_2O_3 + HfO_2$ (b), $Dy_2O_3 + HfO_2$ (c) at D = 50…60 nm (1), 135…138 nm (2), and 1000…2000 nm (3)

A method for the solid-phase synthesis of dysprosium hafnate as a neutron-absorbing material is described in US Patent No. 4992225 [26], in which Dy_2O_3 65...85 wt.% was mixed with HfO_2 and then the resulting mixture was sintered into a compacted sample in the temperature range of 1500...2000 °C in a hydrogen atmosphere.

The main stages of the technological scheme for the synthesis of dysprosium hafnate from the starting oxides and the production of pellets are: mixing of the starting components, briquetting of the fusion mixture by pressing, high-temperature synthesis of dysprosium hafnate, grinding of briquettes and sieving of the powder, cold pressing of pellets, high-temperature sintering of pellets (Fig. 9) [22].

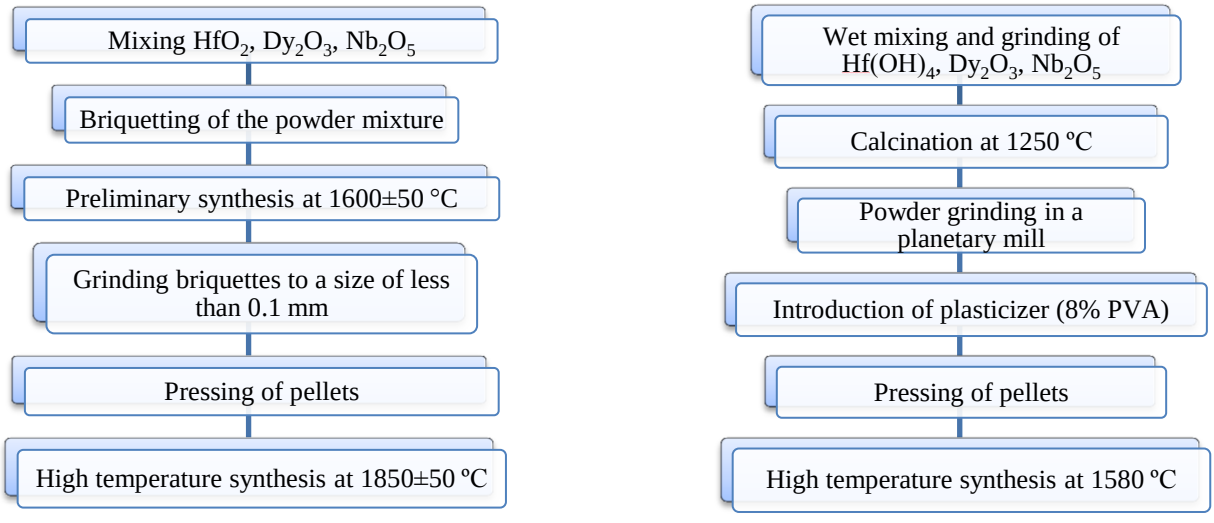

a *b*

Fig. 9. Technological schemes for the production of dysprosium hafnate pellets [24]

According to the first scheme (see Fig. 9,a), hafnium, dysprosium, and niobium oxides are used as starting reagents. According to the second scheme (see Fig.9, b), hafnium hydroxide, dysprosium and niobium oxides are used as starting reagents. The characteristics of dysprosium hafnate pellets after synthesis are given in Tables 3, 4 [24, 27].

Table 3

Results of laboratory development of dysprosium hafnate synthesis technology [27]

Composition	Soaking temperature, °C	Exposure time, h	The result of X-ray powder analysis
Dy_2O_3-23; HfO_2-75; Nb_2O_5-2	1400	1.5	Two FCC fluorite-type structures, traces of starting components
	1500	1.0	FCC fluorite-type structure, traces of Dy_2O_3
	1600	1.0	FCC fluorite-type structure, weak additional lines
	1700	1.0	FCC fluorite-type structure
Dy_2O_3-49; HfO_2-49; Nb_2O_5-2	1400	1.5	FCC fluorite-type structure, weak additional lines
	1500	1.0	FCC fluorite-type structure, weak additional lines
	1600	1.0	FCC fluorite-type structure
	1600	0.5	FCC fluorite-type structure
Dy_2O_3-75; HfO_2-23; Nb_2O_5-2	1400	1.5	FCC fluorite-type structure, C- Dy_2O_3, traces of monoclinic HfO_2
	1500	1.5	FCC fluorite-type structure, traces of starting components
	1600	1.0	FCC fluorite-type structure, traces of starting components
	1700	1.0	FCC fluorite-type structure
	1900	0.5	FCC fluorite-type structure, weak additional lines

Table 4

Results of laboratory development of pellet sintering technology [27]

Molar fraction of components, %	Technological operations	General appearance	Density, g/cm^3	Height and diameter shrinkage characteristics	Structure type	Parameter *a*, nm
Dy_2O_3-23; HfO_2-75; Nb_2O_5-2	Synthesis at 1600 °C, cold pressing, sintering at 1900 °C	No defects	6.86-6.91	Uniform shrinkage 8…11%	Fluorite-type structure	0.51875± 0.00012
Dy_2O_3-49; HfO_2-49; Nb_2O_5-2	Synthesis at (1600±50) °C, cold pressing, sintering at (1800±50) °C		7.11-7.20	Uniform shrinkage 9…12%		0.52311± 0.00012
Dy_2O_3-75; HfO_2-23; Nb_2O_5-2			7.55-7.62	Uniform shrinkage 7…11%		0.51869± 0.00012

The main elements of the technological scheme for the production of dysprosium hafnate pellets based on the results of its development at JSC "ChMZ":

– "wet" process of grinding and mixing of the starting components;

– drying at a temperature of 1250 °C;

- repeated "wet" grinding and drying to an air-dry condition;

– "semi-dry" pressing of pellets with subsequent drying in the air;

– annealing at a temperature of 1580 °C in an air.

A pilot batch of dysprosium hafnate pellets (49 mol.% Dy_2O_3 + 49 mol.% HfO_2 + 2 mol.% Nb_2O_5) with a volume of 6.1 kg (2463 pcs.) was prodced as a result of the technology development.

Results of outgoing inspection of pilot batches of dysprosium hafnate pellets:

– geometric dimensions: diameter – 6.70...6.95 mm, height – 6.5...9.0 mm;

– pellet density: 7.91...8.08 g/cm^3;

– phase composition – fluorite with lattice parameter a = 0.52585 nm.

The RF patent No. 2522747 [28] describes a composition of dysprosium hafnate doped with molybdenum oxide with the following component ratio: Dy_2O_3 60...70 wt.%; HfO_2 25...35 wt.%; MoO_3 3...5 wt.%. At the same time, the starting components used in the preparation of dysprosium hafnate are nanostructured with a coherent scattering region of less than 100 nm. An example of production includes the following technological operations: preparation of a mixture of nanostructured oxides of dysprosium (CSR 35 nm), hafnium (CSR 16 nm) and molybdenum (CSR 67 nm) by wet mixing in a ball mill or other mill at a ratio of masses of the burden and layers of 2:1 for 20 min, briquetting at a pressure of 20...30 MPa and sintering in air at a temperature of 1500...1700 °C for no less than 3 h. As a result, the absorber has the following properties and characteristics: density – 8.1...8.5 g/cm^3, Dy_2O_3 content – 5.0...5.4 g/cm^3; composition: Dy_2O_3-62.3 wt.%; HfO_2-35.2 wt.%; MoO_3-2.5 wt.%; thermal conductivity 1.23 W/(m·K) at 20 °C, CLTE $7.2 \cdot 10^{-6}$ K^{-1}; corrosion resistance: unchanged in distilled water at a temperature of 347 °C and a pressure of 17 MPa. The obtained material was a single-phase ceramic composition based on a solid solution of dysprosium, hafnium, and molybdenum oxides and had an FCC fluorite-type structure.

DYSPROSIUM ZIRCONATE

In [29], the kinetics of a solid solution of Dy_2O_3-$2ZrO_2$ formation was studied. Fig. 10 shows that the binding of Dy_2O_3 to ZrO_2 in a solid solution prevents its crystallization. When Dy_2O_3 interacts with ZrO_2, one reaction product is formed – a cubic solid solution of the fluorite type, the lattice parameter of which changes during the synthesis process: 0.515 nm at 1400 °C (0.5 h) and 0.521 nm at 1400 °C (18 h).

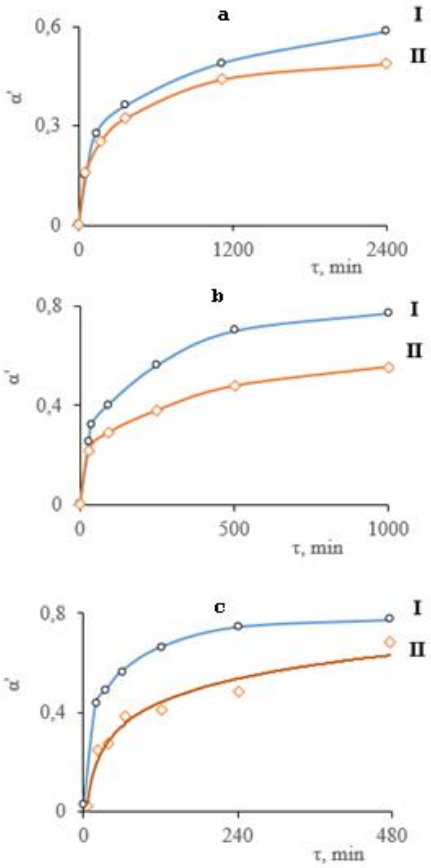

Fig. 10. Kinetic curves of the interaction of the mixture 33.3 mol.% Dy_2O_3 + 66.7 mol.% ZrO_2 at temperatures 1300 (a), 1400 °(b), 1500 °C(c); I – by chemical analysis, II – by X-ray analysis [29]

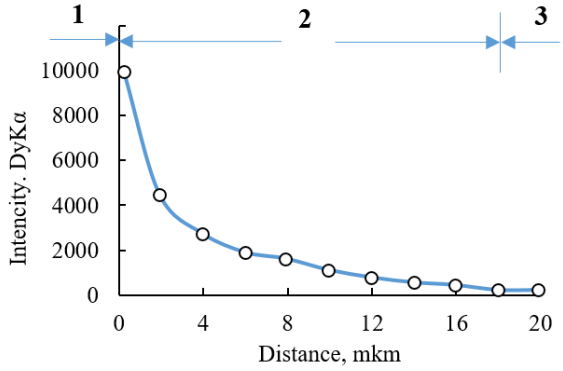

Fig. 11. Distribution of Dy in ZrO_2: 1 – Dy_2O_3; 2 – $Dy_xHf_{1-x}O_y$; 3 – ZrO_2 [29]

Contact diffusion in the Dy_2O_3-ZrO_2 system was studied by X-ray microanalysis to confirm the diffusion mechanism of Dy_2O_3 interaction with ZrO_2. The stacked Dy_2O_3 and ZrO_2 pellets were annealed at 1800 °C for 3 h under a small weighting agent of ZrO_2. Studies have revealed that the interaction is realized mainly through the dysprosium diffusion, resulting in the formation of a solid solution of variable composition $Dy_xHf_{1-x}O_y$ (Fig. 11), which is also confirmed by an increase in the lattice parameter of the solid solution in the process of its formation [29].

INDUCTION MELTING OF OXIDES IN A "COLD" CONTAINER

The method of induction melting of refractory oxides was developed at the P.N. Lebedev Physical Institute and includes three stages [14, 30]: 1) obtaining a "charging" melt; 2) gradual melting under the influence of a high-frequency field of the entire burden except for a thin layer directly adjacent to the water-cooled container wall; 3) slow directed crystallization or lowering of the container against the inductor as shown in Fig. 12.

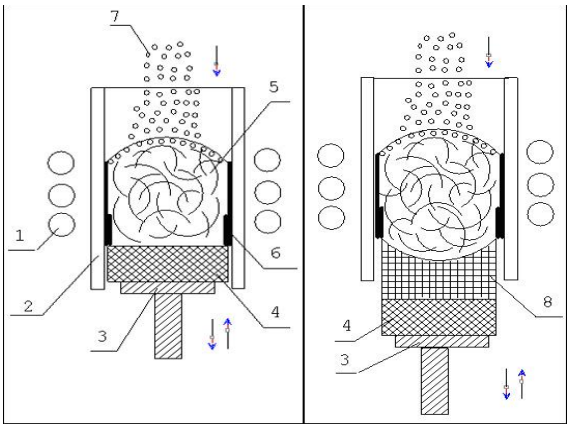

Fig. 12. Scheme of the main elements of induction melting technology: 1 – inductor; 2 – cold melting pot; 3 – retractable bottom; 4 – graphite plate; 5 – melt; 6 – slag lining; 7 – feeding of the starting material from the hopper; 8 – crystallized material

This method was implemented in the synthesis of dysprosium titanate and dysprosium hafnate as a remedy for the disadvantages of heterogeneity and multiphase structure [31–34]. Thus, under the conditions of high-frequency melting of oxides, the process of formation of dysprosium titanate occurs in the liquid phase at temperatures exceeding 2000 °C, which exceeds the melting point of dysprosium titanate and the starting components. In the process of rapid cooling, the high-temperature structure (fluorite face-centered cubic structure) is crystallized, which is the most resistant to radiation exposure. This method of synthesis of dysprosium titanate establishes the composite composition of dysprosium titanate at the ratio of components: Dy_2O_3 (70...85)wt.%+Nb_2O_5 (2...7)wt.%+ZrO_2 (0.5...2)wt.% +TiO_2 – the rest. An increase in the Dy_2O_3 content above 85 wt.% reduces corrosion resistance in water at operating temperatures and pressures under operating conditions. Reducing the Dy_2O_3 content below 70 wt.% can result in the formation of a free titanium phase, which reduces the radiation resistance of dysprosium titanate. The lower limit of the Nb_2O_5 content of 2 wt.% was established based on the absence of its positive effect on the crystal structure of the material obtained by high-frequency induction melting of a mixture of

starting oxides in a cold melting pot. The upper limit of the Nb_2O_5 content (7 wt.%) was established by the requirement to obtain a single-phase material, since at a higher Nb_2O_5 content in the synthesized material at any ratio of other components, an independent phase of dysprosium orthoniobate is formed, which crystallizes in a monoclinic structure, undergoing polymorphic transformations under the influence of irradiation, resulting in a decrease in radiation and corrosion resistance. At a Dy_2O_3 content of more than 78 wt.%, the Nb_2O_5 content should not be less than 5 wt.%, since the introduction of Nb_2O_5 in this case contributes to the expansion of the boundaries of homogeneity regions (solid solutions) and is required to obtain a single-phase material at high Dy_2O_3 content. When the content of ZrO_2 in the material is less than 0.5 wt.%, it has no effect on corrosion resistance under operating conditions. With an increase in the ZrO_2 content of more than 2 wt.%, an independent phase of dysprosium zirconate with a cubic structure is possible to form.

The characteristics of dysprosium titanate pellets obtained by sintering and melting are compared in Table 5.

Table 5

Compositions and characteristics of dysprosium titanate pellets [33]

Production	Sintering technology	Melting technology
Composition, phase	Dy_2TiO_5	Dy_2TiO_5
Crystalline structure	Hexagonal a=(0.3636±0.0002) nm, c=(1.1843±0.0005) nm	Fluorite a=(0.5200±0.0001) nm
Pellets density, g/cm^3	5.9…6.1	6.1…6.2
Thermal conductivity, W/(m·K)	1.0 (25°C); 1.5 (800°C)	-
CLTE, $\times10^{-6}$ K^{-1}	6.5 (25°C); 8.7 (400°C)	-
Microhardness, MPa	7000±1000	12000±1000
Strength limit, MPa	100…130 (20 °C)	100…130 (20 °C)

The structures of sintered and melted dysprosium titanate absorbers differ significantly (Fig. 13). Sintered dysprosium titanate is characterized by porosity evenly distributed over the entire cross-section of the pellet with a pore size of 80 to 100 μm. Melted dysprosium titanate contains large particles with a size of about 250 μm.

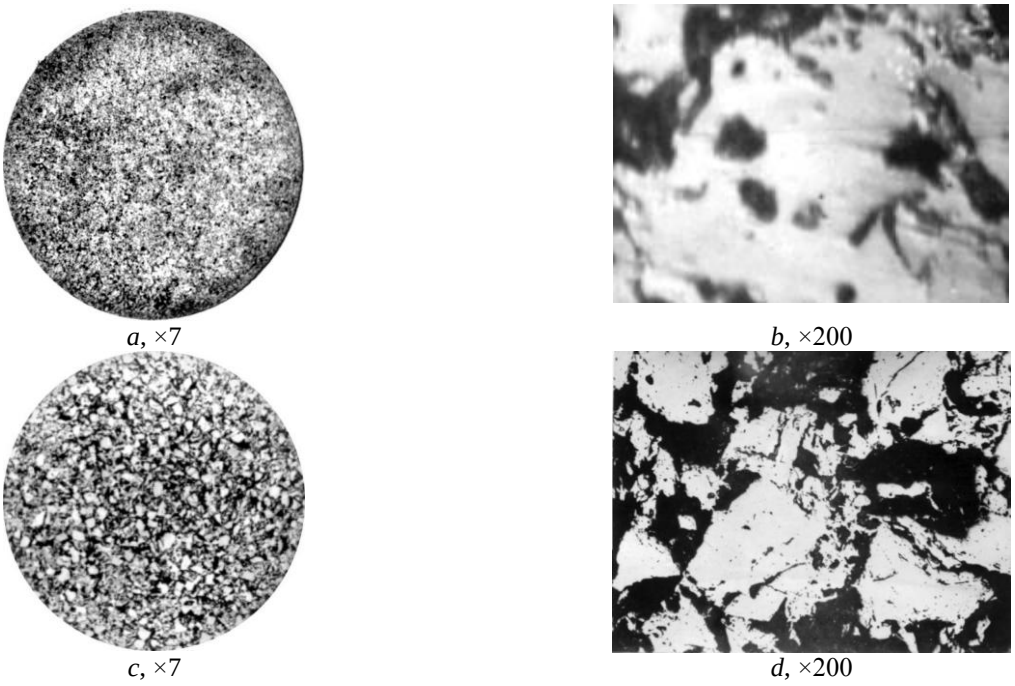

a, ×7 *b*, ×200

c, ×7 *d*, ×200

Fig. 13. Macro- (a, c) and microstructures (b, d) of sintered (a, b) and melted (c, d) dysprosium titanate pellets [33]

This method was also implemented in the synthesis of dysprosium hafnate with a fluorite-type structure in a wide range of concentrations of the starting components: Dy_2O_3 (12...85) wt.%+HfO_2 (0.5...87) wt.%+ Nb_2O_5 (0.5...20)wt.% [31]. Thus, the stabilization of the fluorite structure is ensured by the presence of niobium oxide in the starting reagents. Moreover, the lower limit of Nb_2O_5 content of 0.5 wt.% is caused by the absence of its positive effect on the crystal structure of the material obtained and on the technological parameters of synthesis by high-frequency induction melting of the oxides mixture. The upper limit of the Nb_2O_5 content of 2 wt.% is required to obtain a solid solution with a face-centered cubic lattice of the fluorite type. When the

content of niobium oxide exceeds 20 wt.% in the synthesized material at any ratio of other components, an independent phase of dysprosium orthonyobate is formed, crystallizing in a monoclinic structure, which undergoes polymorphic transformations under the influence of reactor irradiation, resulting in a significant decrease in its radiation and corrosion resistance. The upper limit of the Dy_2O_3 content of 85 wt.% is limited by the formation of the second phase – Dy_2O_3, which significantly reduces the corrosion resistance of the proposed material in water of high parameters. With a Dy_2O_3 content of less than 12 wt.%, a second phase with a monoclinic structure based on HfO_2 is formed, which undergoes polymorphic transformations with a volume increase of ~7% under the influence of reactor irradiation. With a Dy_2O_3 content above 78 wt.%, the Nb_2O_5 content should be at least 5 wt.%.

Characteristics of dysprosium hafnate pellets obtained by melting technology are given in Table 6.

Table 6

Characteristics of pellets of melted dysprosium hafnate [4, 24]

Compositions of dysprosium hafnate	Dy_2O_3-75; HfO_2 -23; Nb_2O_5 -2	Dy_2O_3·-49; HfO_2-49; Nb_2O_5-2	Dy_2O_3·-23; HfO_2-75; Nb_2O_5-2
Crystalline structure	Fluorite a=(5.1875±0.0012) Å	Fluorite a=(5.2311±0.0012) Å	Fluorite a=(5.1869±0.0012) Å
Density, g/cm^3	6.8…7.1	7.0…7.2	7.4…7.8
Thermal conductivity, W/(m·K)	2.0 (25 °C)	1.5 (25 °C)	1.7 (25 °C)
CLTE, $\times 10^{-6}$ K^{-1}	8.54 (25…100 °C) 11.58 (500 °C)	8.66 (25…100 °C) 11.05 (500 °C)	8.37 (25…100 °C) 11.47 (500 °C)
Microhardness, MPa	7000…13000		
Compressive strength limit, MPa	150 (20 °C) 80 (500 °C)	350 (20 °C) 130 (350 °C)	350 (20 °C) 170 (350 °C)

CHEMICAL METHODS

Recently, research and development of low-temperature methods for the synthesis of absorbing materials based on rare earth elements has intensified, among which are the methods based on the decomposition of salts or high molecular weight organic polymers [36–38], as well as chemical deposition of hydroxides followed by annealing [39–41].

As a rule, amorphous hydroxides are deposited under the influence of an aqueous solution of ammonia-containing reagents (NH_3) on nitric acid or hydrochloric acid solutions of titanium and dysprosium. The resulting products are filtered, washed, dried at 100 °C and subjected to heat treatment. Generally, the resulting precipitates are X-ray amorphous and contain a significant amount of chemically bound rare earth hydroxide [14]. Crystalline titanates of rare earth elements are formed upon further heating up to the crystallization temperature.

Korean researchers have performed a comparative study of the characteristics of dysprosium titanate pellets obtained both by chemical method (ethylene glycol – EG-process) and by standard solid state synthesis (SS-process) [36].

A distinctive feature of the EG-process is that the starting reagents used are titanium and dysprosium salts, which were dissolved in ethylene glycol. The transparent solution was dried for 48 h at 80 °C to form a gel. Subsequently, annealing at different temperatures for 1 h and grinding in a ball mill for 6 h to eliminate agglomerates were performed. The resulting powder was compacted at a pressure of 30 MPa and sintered in air at different temperatures. Powders calcined for 1 h at temperatures below 800 °C possess an X-ray amorphous structure. The orthorhombic phase is formed as a result of calcination for 1 h to a temperature of 1300 °C. A further increase in temperature results in the formation of a hexagonal structure. The powders obtained by the EG-process are characterized by a high specific surface area and a smaller particle size compared to the powders obtained by the standard technology (Table 7).

Table 7

Specific surface and particle size of Dy_2TiO_5 powder [36]

Process	Specific surface, g/cm^3	Particle size, μm
EG	14.0	0.38
SS	3.5	1.52

The microstructures of the sintered pellets obtained by the EG-process (sintering for 2 h) and the SS-process (sintering for 10 h) at temperatures of 1500 and 1600 °C, respectively, are presented in Fig. 14.

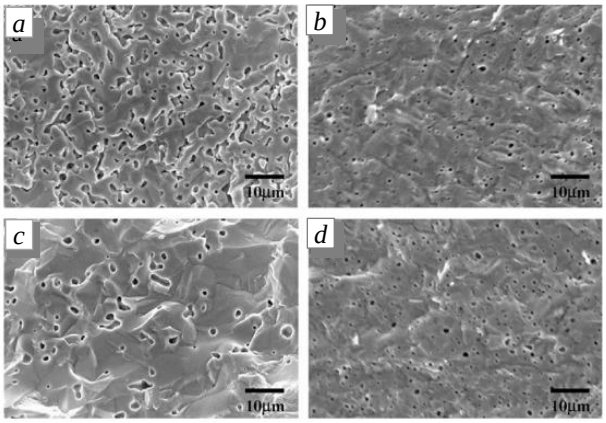

Fig. 14. Microstructure of sintered Dy_2TiO_5: SS-process (a), EG-process (b) at 1500 °C (c) and 1600 °C (d), respectively [36]

The sample sintered at 1500 °C (see Fig. 14,a) contains long pore channels and irregularly shaped grains (density 6.21 g/cm^3, 85% of the theoretical density). Sintering at 1600 °C resulted in rapid grain enlargement

and the formation of large and unevenly shaped pores. In the case of sintering the samples obtained by the EG-process at 1500 °C, a density of 6.93 g/cm^3 was achieved, which is 95% of the theoretical one, but small pores remained. The microstructure of Dy_2TiO_5 pellets sintered at 1600 °C obtained by the EG-process (density of 7.04 g/cm^3) was characterized by a grain size of 3...5 μm with small pores at the boundaries (see Fig. 14,d).

According to the method for obtaining ceramic materials based on nanocrystalline powders of dysprosium hafnate, the production of mixed dysprosium and hafnium hydroxides is carried out by dissolving the salts $HfOCl_2 \cdot 8H_2O$ and $Dy(NO_3)_3 \cdot 5H_2O$ in water and adding the resulting solution to an ammonia solution, filtering and washing the resulting precipitate, drying with subsequent calcination to obtain dysprosium hafnate, its grinding, pressing and annealing of the resulting compacts, characterized in that the stage of drying and calcination of the mixed hydroxide is carried out under the influence of microwave heat with a continuous power of 1.5…6.0 kW, gradually changing the temperature during 1.0...1.5 h to obtain nanocrystalline dysprosium hafnate powder.

The obtained dysprosium hafnate powders after drying at 90 °C for 12 h and calcination in air at 800 °C for 3.0 h exhibited a nanocrystalline size of the coherent scattering regions of 9 nm and an FCC structure of the fluorite type. Dy_2HfO_5 powder mechanically activated for 33 min exhibited a specific surface area of 10.4 m^2/g. The density of the pellets was 4.71 g/cm^3 after pressing at 180 MPa. Sintering of the pellets at a temperature of 1550 °C for 4 h resulted in an increase in the density of the pellets to 8.0 g/cm^3.

The main results of the research into the phase formation of dysprosium hafnate with a composition of 63.9 wt.% Dy_2O_3 + 36.1 wt.% HfO_2 (50 mol.% Dy_2O_3 + 50 mol.% HfO_2) obtained by calcination of the thermal decomposition products of co-precipitated hafnium and dysprosium salts are given in [41]. According to the results of DTA and TG analyzes of the product of chemical co-precipitation of hafnium and dysprosium salts, it was observed that the maximum rate of molecular water removal occurs at 150 °C (endothermic effect at 150 °C) (Fig. 15).

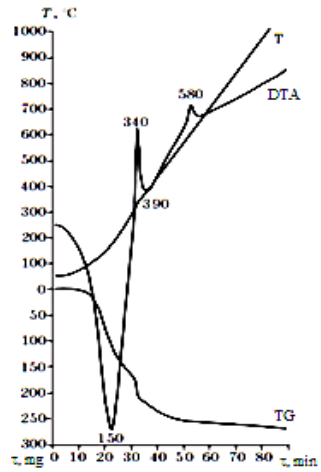

Fig. 15. Thermal and gravimetric patterns of dysprosium hafnate hydroxide decomposition [41]

Two exothermic effects at 340 and 580 °C were observed, which may indicate the crystallization of dysprosium hafnate.

The weight change of sample was already insignificant at temperatures above 580 °C and no exothermic effects were observed up to a temperature of 1000 °C, indicating that the crystallization process of dysprosium hafnate was completed. According to the results of X-ray diffraction analysis, it was established that in the process of joint chemical precipitation of hydroxides from nitric acid salts of hafnium and dysprosium, an X-ray amorphous precipitate is formed (Fig. 16).

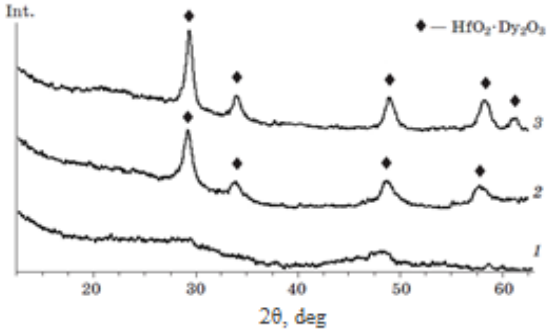

Fig. 16. Diffractograms of thermal decomposition products of dysprosium hafnate hydroxide in the starting condition (1) and after heat treatment for 1 h at 700 °C (2) and 1000 °C (3) [41]

It was observed that calcination at a temperature of 700 °C results in the formation of dysprosium hafnate with a cubic lattice of the fluorite type with parameters of (0.518±0.001) nm and crystallite sizes of 20...40 nm. Increasing the calcination temperature to 1000 °C results in an increase in crystal size to 40...60 nm.

MECHANOCHEMICAL ACTIVATION

In recent years, research into the synthesis of titanates and hafnates of rare earth elements, primarily dysprosium and gadolinium, by mechanochemical treatment using ball planetary mills has been significantly intensified: Dy_2TiO_5 [42–47], Dy_2HfO_5 [48], Gd_2HfO_5 [49], $Gd_2Ti_2O_7$ [50].

Thus, a method for obtaining highly dispersed dysprosium titanate powders includes the preparation of dysprosium titanate powder by mechanical activation of a mixture of components – titanium dioxide – TiO_2 and dysprosium oxide – Dy_2O_3, taken in an equimolar ratio, in a planetary ball mill at a planetary disk rotation speed of 100…900 rpm, drum rotation speed of 1000…2400 rpm, with a ball weight to burden weight ratio of 45:1 in an argon atmosphere at P = 3…5 atm for 20…60 min [51].

The mechanochemical treatment of titanium and dysprosium oxides for 30…60 min resulted in the complete transformation of the initial oxides into dysprosium titanate (amorphous structure) [42]. After 60...90 min of treatment, traces of iron were observed as a result of rubbing of the grinding layers. The specific surface area of the powders was 12.0...32.4 m^2/g. Nanoscale particles of dysprosium titanate powder of non-equilibrium shape with a size of 50...200 nm, which were combined in agglomerates up to 0.5...10 μm, were obtained.

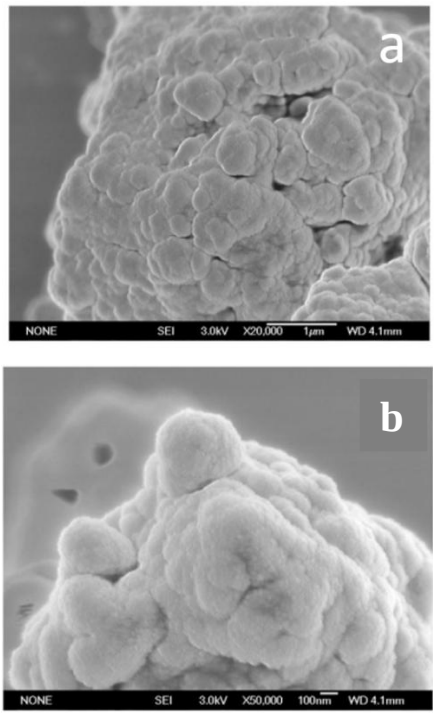

Fig. 17. Mechanosynthesized product: a – agglomerates; b – nanoparticles that form agglomerates [42]

Combining the methods of chemical precipitation and mechanoactivation also enabled the production of dense dysprosium hafnate pellets with a monophase structure [40]. The method involves the production of mixed hydroxide by co-precipitation of salts, filtration and washing of the resulting precipitate, drying followed by calcination to obtain mixed oxide, its grinding, pressing and sintering of pellets. Thus, the calcination stage of the mixed hydroxide is carried out in the temperature range of 800...1200 °C, and the grinding of mixed oxide powders is carried out by mechanical activation in a planetary mill for 18...36 min. The dysprosium hafnate powders obtained by calcination in a muffle furnace in air for 3 h at a temperature of 800...600 °C had a single-phase composition – Dy_2HfO_5, which had an FCC structure of the fluorite type, with crystallite sizes depending on the treatment temperature (Table 8).

Table 8

Production modes and characteristics of dysprosium hafnate nanopowders [40]

Temperature, °C	Crystallite size, nm	Parameter, Å	Micro-stresses, %
400	amorphous	–	–
600	amorphous	–	–
800	8	5.258	1.6
1000	18	5.2570	0.6
1200	62	5.2602	0.3
1400	270	5.2604	0.1
1600	330	5.2622	<0.1

One can see that an increase in the calcination temperature above 1200 °C results in a sharp increase in the size of crystallites and the formation of large-crystalline Dy_2HfO_5 powders. Several batches of pellets were produced from nanocrystalline dysprosium hafnate powder with a crystallite size of 8 nm, which was obtained by-calcination of hydroxides at 800 °C for 3 h, which differed by the time of mechanical activation in a planetary mill.

The pressing pressure was 180 MPa, and the sintering temperature and time were 1550 °C and 4 h, respectively. Table 9 presents data on the dependence of the density of sintered pellets on the time of mechanical activation.

Table 9

Density of sintered dysprosium hafnate pellets [40]

Mechanoactivation time, minutes	15	36	48
Density of pellets, g/cm^3	7.30	7.96	7.97

In the work of Chinese researchers, it was observed that the treatment of a powder mixture of TiO_2 and Dy_2O_3 in a planetary mill at 500 rpm results in a significant reduction in grain size (up to 60 nm) and transformation of the crystal lattice of dysprosium oxide with the formation of an X-ray amorphous structure [52]. Mechanoactivation under these conditions for 96 h resulted in the complete destruction of the crystal structures of the starting oxides and amorphization of the mixture.

The calcination of mechanical treatment products at temperatures in the range of 800...1000 °C resulted in the formation of a metastable dysprosium dititanate structure $Dy_2Ti_2O_7$ with a cubic lattice, which at higher temperatures transforms into an equilibrium orthorhombic lattice Dy_2TiO_5.

XRD patterns of the Dy_2O_3-TiO_2 powder mixtures milled at 500 and 200 rpm for different grinding times are given in Fig. 18. The XRD results show that the crystal structure of the starting Dy_2O_3 phase and the TiO_2 phase are cubic and rutile, respectively. At 500 rpm, the diffraction peaks of cubic Dy_2O_3 and TiO_2 broaden significantly and decrease in intensity with increasing grinding time. The broadening of the X-ray diffraction peaks is associated with the grinding of the grain size and the decay of the crystal lattice.

High-rate grinding results in the transformation of Dy_2O_3 from a cubic to a monoclinic crystal structure. A broad diffraction peak indicates the formation of an amorphous phase during ball milling. The fact that the amorphous peak is present at the position of the diffraction peak for monoclinic Dy_2O_3, but not at the position of the diffraction peak for the cubic Dy_2O_3 phase, indicates that the formed amorphous phase is derived from the monoclinic Dy_2O_3 phase, and not from cubic Dy_2O_3.

After milling for 96 h, only the amorphous phase was observed, indicating that the monoclinic phase of Dy_2O_3 was completely transformed into the amorphous phase (see Fig. 18,a). In addition, this behavior indicates that no new compounds are synthesized during ball milling. The behavior of the powder mixtures during ball milling at 200 rpm was significantly different from that at 500 rpm. The change in the diffraction peaks with increasing grinding time at 200 rpm is given in Fig. 18,b. Although the diffraction peaks of cubic Dy_2O_3 and TiO_2 also broaden and decrease in intensity with increasing grinding time, the diffraction peaks of TiO_2 were observed in the XRD patterns and did not disap-

pear. After grinding for 96 h, the intensity of the diffraction peaks of Dy_2O_3 and TiO_2 also remained high. The powder mixtures did not change completely before amorphization. Thus, at low ball mill rotation rates, the powder mixtures were only ground and homogenized.

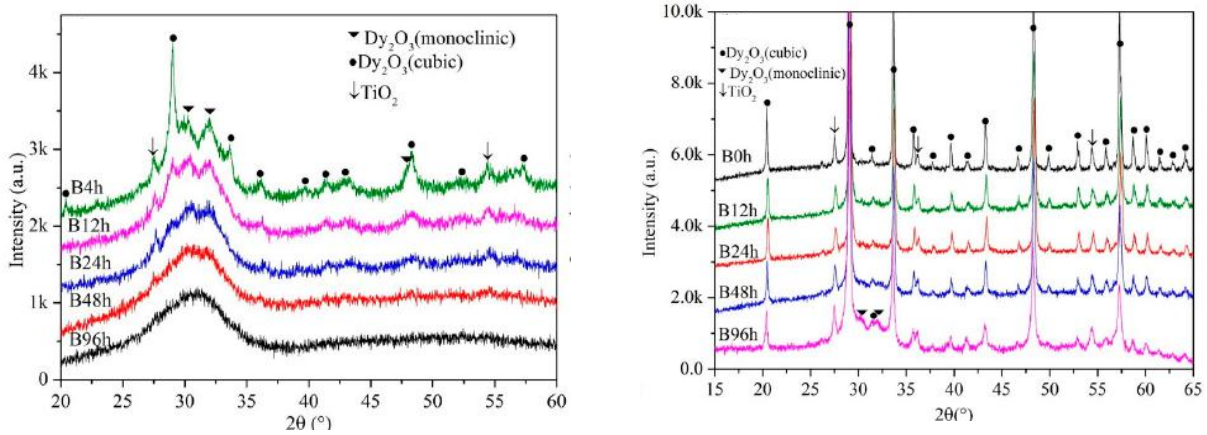

Fig. 18. X-ray diffraction patterns of powder mixtures milled at 500 (a) and 200 rpm (b) for different times, respectively [52]

The results of the XRD analysis of powder mixtures milled for 96 h and annealed at 800, 900, 1000, 1050, 1100, and 1150 °C are presented in Fig. 19. Several diffraction peaks differ from the diffraction peaks of Dy_2O_3 (cubic and monoclinic crystal structure) and TiO_2 (rutile structure), indicating the formation of new components with crystal structures that were formed from amorphous mixtures.

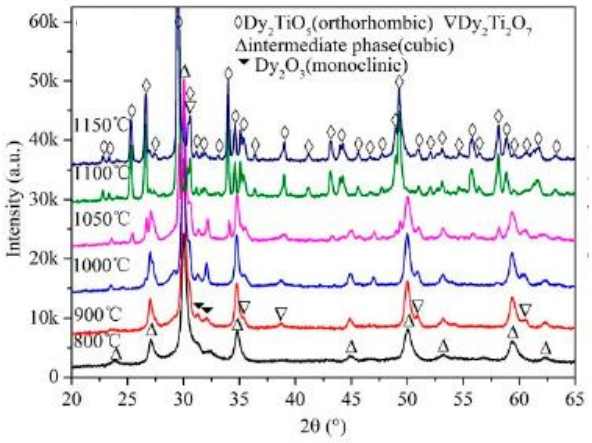

Fig. 19. X-ray diffraction patterns of powder mixtures annealed for 3 h at different temperatures [52]

The XRD patterns of Dy_2O_3-TiO_2 powder mixtures showed three diffraction peaks at temperatures of 800, 900, and 1000 °C: orthorhombic Dy_2TiO_5, cubic pyrochlore $Dy_2Ti_2O_7$, and cubic fluorite Dy_2TiO_5 (see Fig. 19). The latter phase was an intermediate and metastable phase that transformed into orthorhombic Dy_2TiO_5 at an annealing temperature above 1050 °C.

The research into the phase transformations during the mechanical grinding of mixtures based on titanium, gadolinium, and dysprosium oxides, performed by scientists from the Republic of Mexico, also confirmed the formation of a significant number of structural defects and the transformation of cubic dysprosium and gadolinium oxides into a monoclinic structure [53]. Thus, the mechanochemical treatment of materials for 9 h resulted in the formation of a high-temperature modification of Gd_2TiO_5 with a hexagonal structure. Differential thermal analysis also revealed a phase transformation at a temperature of about 800 °C. Treatment at 1100 °C resulted in the formation of a low-temperature modification of Gd_2TiO_5 with an orthorhombic structure.

PLASMOCHEMICAL SYNTHESIS

All known plasmochemical methods of producing and synthesizing of powders can be combined into three methods based on the aggregate state of the starting material introduced into the plasma [54]:

1) processing of gaseous compounds;

2) processing of drip-liquid raw materials;

3) processing of solid particles suspended in the plasma flow.

Since both liquid and solid raw materials are converted to gaseous state in plasma, all three methods can be classified as gas-phase condensation methods.

For example, in [55], ZrO_2 nanopowders were obtained by oxidizing dispersed $ZrCl_4$ with a limited jet flow based on an electric arc plasmatron. Changing the flow rate of $ZrCl_4$ and the enthalpy of the plasma flow enabled the production of nanopowders with a specific surface area of 18…32 m^2/g (with an average grain size of 33…58 nm). The obtained nanopowders were polydisperse, consisted of equiaxed particles of rounded shape, and contained 0.25…0.75 wt.% of chlorine.

Paper [56] describes the processing of a neutron-absorbing material in the form of gadolinium oxide (Gd_2O_3) in an HF plasmatron, which results in the spheroidization of the starting particles of the powdered material in the plasma flow. The development of variously grained crystals with a grain size of 0.008…0.02 mm, with a normal optical characteristics and a predominance of columnar crystals was observed. The mechanism of plasma effect on particles is quite complex. The main influencing factor is thermal heating by plasma, the temperature of which can reach more than 5000 °C in the current-carrying channel, and the heating rate is 104 deg/s. During the period of particles' exposure in the plasma, which ranges from 0.3 s in the case of unidirectional movement of particles and plas-

ma-forming gas and up to 2 s in the case of processing large particles in the counterflow of gas, the particles reach the melting point.

The patent [57] describes a method for obtaining microspherical powders of dysprosium titanate with a composition of 50 mol.%. Dy_2O_3 - 50 mol.% TiO_2 and dysprosium hafnate with the composition of 50 mol.% Dy_2O_3-50 mol.% HfO_2 that ensures the production of an equimolar mixture of oxides, trapping the resulting powder particles and their annealing.

The product from all batches of titanate-dispersed compositions consisted of a morphological array of similar particles with a predominance of void spheres, with an average size of 200 nm. The sizes of the crystallites included in the spheres were in the range of 10…60 nm.

No changes in the crystal structure of titanium-dysprosium oxide compositions were observed when heated to 1000 °C. When heated from 1050 to 1600 °C, the structure of this material changed from a cubic phase, such as fluorite, to a hexagonal phase.

CONCLUSIONS

1. A review of the known methods for the synthesis of titanates, hafnates, and zirconates of rare earth elements, which have been applied as neutron-absorbing materials for nuclear reactors and are promising due to their high radiation and corrosion resistance, has been carried out.

2. Among the considered methods, the most widely used in the production of dysprosium titanate and dysprosium hafnate were the method of solid-phase synthesis and methods of induction melting of the starting oxide mixtures. The general mechanism of solid-phase synthesis of dysprosium titanate and dysprosium hafnate is preferential diffusion with the formation of intermediate chemical compounds or solid solutions.

3. The NFC STE NSC KIPT is carrying out R&D to study the effect of technological operation parameters on the synthesis and characteristics of dysprosium titanate and dysprosium hafnate pellets with a controlled structural and phase condition.

REFERENCES

1. Accident-tolerant control rods // *State-of-the-art report on light water reactor accident-tolerant fuels* NEA No. 7317, OECD 2018.

2. V. Ponomarenko et al. WWER-1000 Control Rod Materials: Experience and development // *IAEA-TECDOC-1132. Control assembly materials for water reactors: Experience, performance and perspectives. Proceedings of a Technical Committee meeting held in Vienna*, 12-15 October 1998, p. 175-189.

3. V.D. Risovaniy et al. Dysprosium and hafnium base absorbers for advanced WWER control rods // *IAEA-TECDOC-1132. Control assembly materials for water reactors: Experience, performance and perspectives. Proceedings of a Technical Committee meeting held in Vienna*, 12-15 October 1998, p. 91-102.

4. V.D. Risovany et al. Dysprosium hafnate as absorbing material for control rods // *Journal of Nuclear Materials*. 2006, v. 355. p. 163-170.

5. V.M. Chernyshov et al. *Control rod of water-cooled vessel reactor*: Patent Ukraine 29541, G21C7/24, №a99084723; filing date 18.02.1997; published 15.11.2000.

6. V.M. Chernyshov et al. *Control rod in a water-cooled nuclear reactor*: European Patent 0977206B1, G21C 7/10, G21C 7/24, G21C 7/103; filing date 15.11.2000; published 16.07.2003.

7. V.D. Risovaniy et al. New generation absorbing materials for thermal neutron power reactors // *Problems of Atomic Science and Technology.* 2020, N 4, p. 82-93.

8. V.G. Shamrai at al. System Dy_2O_3-TiO_2 // *Proceedings of the USSR Academy of Sciences. Ingranic Materials.* 1989, v. 25, N 2, p. 273-275.

9. M.A. Petrova, A.S. Novikova, R.G. Grebenshchikov. Polymorphism of rare-earth element titanates of composition Ln_2TiO_5 // *Proceedings of the USSR Academy of Sciences. Ingranic Materials*. 1982, v. 18, N 2, p. 287-291.

10. Ye.B. Petrova, F.M. Spiridonov, L.N. Komissarova Phase equilibria in the system HfO_2-Dy_2O_3 // *Proceedings of the USSR Academy of Sciences. Ingranic Materials*. 1972, v. 8, N 10, p. 1878.

11. A.V. Shevchenko, L.M. Lopato, L.V. Nazarenko. Systems of HfO_2 with oxides of samarium, gadolinium, terbium and dysprosium at high temperatures // *Proceedings of the USSR Academy of Sciences. Ingranic Materials*. 1984, v. 20, N 11, p. 1862-1866.

12. O.A. Kornienko, E.R. Andriyivska, J.D. Bogatyreva, S.F. Korichev. Phase equilibria in the ZrO_2-Dy_2O_3 system at 1100, 1500 °C // *Bulletin of Kharkiv National University*, 2016, v. 27 (50), p. 39-48.

13. P. P. Fedorov, E. V. Chernova. Conditions of solid-phase synthesis of solid solutions in systems of zirconium and hafnium dioxides with oxides of rare-earth elements // *Condensed Media and Interphase Boundaries*. 2022, N 24(4), p. 537–544.

14. P.A. Arseniev et al. *Compounds of rare earth elements. Zirconates, gafnates, niobates, tantalates, antimonates.* M,: "Nauka". 1985, p. 261.

15. Robert D. Aughterson, Nestor J. Zaluzec, Gregory R. Lumpkin. Synthesis and ion-irradiation tolerance of the Dy_2TiO_5 polymorphs // *Acta Materialia.* 2021, v. 204, p. 1-10.

16. Amit Sinha, B.P. Sharma. Development of Dysprosium. Titanate Based Ceramics for Control Rod Application // *Journal of the American Ceramic Society.* 2005, v. 88, issue 4, p. 1061-1066.

17. L.G. Shcherbakova, L.G. Mamsurova, G.E. Sukhanova. Titanates of rare-earth elements // *Advances in chemistry*. 1979, N 48, p. 423-447.

18. V.D. Risovany, Ye.Ye. Varshalova, D.N. Suslov. Dysprosium titanate as an absorber material for control rods // *Journal of Nuclear Materials*. 2000, v. 281, p. 84-89.

19. Kevin Seymour, Scott James Mccormack, Waltraud M. Kriven, Daniel Ribero. Relationship Between the Orthorhombic and Hexagonal Phases in Dy_2TiO_5 // *Journal of the American Ceramic Society*. 2016, v. 99, N 11, p. 3739-3744.

20. G.C. Lau, B.D. Muegge, T.M. McQueen, E.L. Duncan, R.J. Cava. Stuffed rare earth pyrochlore

solid solutions // *Journal of Solid State Chemistry.* 2006, v. 179, issue 10, p. 3126-3135.

21. I.A. Chernov, N.N. Belash, I.V. Kolodiy, E.B. Valezhny. A.S. Kalchenko, E.A. Slabospitskaya. Phase formation and characteristics of tablets based on dysprosium titanate-nate at solid-phase synthesis // *Problems of Atomic Science and Technology*. 2017, N 2, p. 150-155.

22. I.O. Chernov, M.M. Belash, V.O. Romankov, O.O. Slabospytska, I.V. Kolodiy, and O.S. Kalchenko. Effect of MoO_3 and TiO_2 powder particle sizes on the phase composition and density of dysprosium titanate pellets // *Powder Metallurgy and Metal Ceramics.* 2023, N 62(3-4), p. 257-264.

23. V.B. Glushkova et al. Study of kinetics of the initial stages of formation of compounds and solid solutions in the system Ln_2O_3 – HfO_2 (Ln–Nd, Sm, Dy) // *Proceedings of the USSR Academy of Sciences. Ingranic Materials*. 1976, v. 12, N 4, p. 695.

24. V.D. Risovaniy et al. *Dysprosium in Nuclear Engineering.* Dimitrovgrad, 2011, 224 p.

25. V.B. Glushkova et al. Study of the influence of the degree of dispersion of HfO_2 on its interaction with Ln_2O_3 // *Inorganic materials*. 1975, v. 11, N 5.

26. *Water corrosion-resistant ceramic oxide body*: United States Patent 4992225. Cl. F27B 9/04. filing date Oct. 19. 1988, published Feb. 12. 1991.

27. A.V. Zakharov et al. Properties of dysprosium hafnate as an absorbing material for controlling organs of prospective thermal neutron reactors for mass production of pellets // *Proceedings of research institute of nuclear reactors*. 2009, issue 4, p. 32-34

28. V.K. Nevorotin, V.F. Petrunin, V.V. Popov. *Neutron-absorbing material based on dysprosium hafnate:* Patent No. 2522747, published 20.07.2014.

29. V.B. Glushkova, V.A. Krizhanovskaya, E.K. Keller. Kinetics of Dy_2O_3-ZrO_2 solid solution formation // *Proceedings of the USSR Academy of Sciences. Ingranic Materials*. 1973, v. 9, N 4, p. 739.

30. V.I. Aleksandrov, V.V. Osiko, A.M. Prokhorov, V.M. Tatarintsev. A new method for obtaining refractory single crystals and fused ceramic materials // *Bul. AS USSR*, 1973, 12, p. 29-36.

31. A.V. Zakharov et al. *Neutron-absorbing material:* RF Patent №2142654, published 10.12.1997.

32. V.D. Risovaniy et al. *Neutron absorber for nuclear reactors*: RF Patent No. 2124240, published on December 27, 1998.

33. V.M. Chernyshov et al. *Material absorbing neutrons:* RF Patent No. 2080667, published on 27.05.1997.

34. A.V. Zakharov et al. *Neutron absorber for control rods of nuclear reactors:* RF Patent No. 2101789, published on January 10, 1998.

35. V.D. Risovanyi, A.V. Zakharov, E.M. Muraleva. New perspective absorbing materials for nuclear reactors on thermal neutrons // *Problems of Atomic Science and Technology*. 2005, N 3(86), p. 87-93.

36. Xue Guo, Yurun Feng, Jiaxing Zhao, Li Ma, Qisong Li, Zhang Zhang, Hongyu Gong, Yujun Zhang, Neutron absorption performance of Dy_2TiO_5 materials obtained from powders synthesized by the molten salt method // *Ceramics International* 2017, v. 2, issue 43, p. 1975-1979.

37. Choong-Hwan Jung, Chan-Joong Kim, Sang-Jin Lee. Synthesis and sintering studies on Dy_2TiO_5 prepared by polymer carrier chemical process // *Journal of Nuclear Materials*. 2006, N 354, issue 1-3, p. 137-142.

38. Zhang Weiguang, Lili Zhang, Hui Zhong, Lude Lu, Xujie Yang, Wang Xin Synthesis and characterization of ultrafine $Ln_2Ti_2O_7$ (Ln=Sm, Gd, Dy, Er) pyrochlore oxides by stearic acid method // *Materials Characterization*. 2010, v. 61, N 2, p. 154-158.

39. D. Alyoshin et al. Preparation of HfO_2-Dy_2O_3-Nb_2O_5 composite powders by chemical precipitation from solutions // *Politechika Krakowska.* 2008, p. 7-17.

40. V. Popov et al. RF Patent No. 2467983, Method of preparation of nanocrystalline powders of dysprosium hafnate and ceramic materials on their basis, published 20.10.2015.

41. N.N. Belash, I.A. Chernov, N.V. Rud, R.A. Rud, A.V. Kushtym, F.V. Belkin. Investigation of pro-processes of obtaining nanocrystalline powders HfO_2, Dy_2O_3 and Dy_2O_3-HfO_2 and dysprosium hafnate pellets with their use // *Collection of scientific papers of PJSC "Ukr. Research Institute of Refractories named after A.S. Berezhnyi"*. 2014, N 114, p. 82-90.

42. Zh.V. Eremeeva, V.S. Panov, L.V. Myakisheva, A.V. Lizunov, A.A. Nepapushev, D.A. Sidorenko, S. Vorotilo. Structure and properties of mechanochemically synthesized dysprosium titanate Dy_2TiO_5 // *Journal of Nuclear Materials*. 2017, v. 495, p. 38-48.

43. Jinhua Huang, Guang Ran, Jianxin Lin, Qiang Shen, Penghui Lei, Xina Wang, and Ning Li. Microstructural Evolution of Dy_2O_3-TiO_2 Powder Mixtures during Ball Milling and Post-Milled Annealing // *Materials*, 2017, issue 10, p. 1-12.

44. G. Garcia-Martinez, L.G. Martinez-Gonzalez, J.I. Escalante-Garcıa, A.F. Fuentes. Phase evolution induced by mechanical milling in Ln_2O_3:TiO_2 mixtures (Ln=Gd and Dy) // *Powder Technology.* 2005, v. 152, issue 1-3, p. 72-78.

45. V.S. Panov et al. Study of the process of obtaining nanostructured disprosium titanate by mechanochemical treatment of titanium and dysprosium oxides // *Proceedings of South-West State University*. 2015, N 5(62), p. 21-26.

46. J.V. Eremeevaa, S. Vorotilo, D.Yu. Kovalev, A.A. Gofman, and V. Y. Lopatin. Mechanochemical Synthesis of Dy_2TiO_5 Single-Phase Crystalline Nanopowders and Investigation of Their Properties // *Inorganic Materials: Applied Research.* 2018, v. 9, N 2, p. 291-296.

47. J.V. Eremeeva et al. Structure and properties of dysprosium titanate powder obtained by mechanochemical method // *Izvestiya Vuzov. Powder Metallurgy and Functional Coatings*. 2017, N 1, p. 11-19 (in Russian).

48. Zh.V. Eremeeva, Yu.Yu. Kaplanskiy, S. Vorotylo, A.A. Nepapushev, D.A. Sidorenko, A.V. Khvan. Fabrication of Nanodispersed Powder of Dysprosium Hafnate Dy_2HfO_5 by Mechanochemical Method // *Inorganic Materials: Applied Research*. 2021, v. 12, issue 4, p.1042–1046.

49. J.V. Eremeyeva et al. Preparation of nanodisperse powder gadolinium gafnate Gd_2HfO_5 mechano-

chemical method // *Eurasian Union of Scientists* (EUU) # 9(78). 2020, p. 23-28.

50. P.K. Kulriya, Tiankai Yao, Spencer Michael Scott, Sonal Nanda, Jie Lian. Influence of grain growth on the structural properties of the nanocrystalline $Gd_2Ti_2O_7$ // *Journal of Nuclear Materials*. 2017, v. 487, p. 373-379

51. V.S. Panov et al. *Method for obtaining dysprosium titanate powder for absorbing elements of a nuclear reactor*: Patent RU 2590887, publ. 10.07.2016.

52. Jinhua Huang, Guang Ran, Jianxin Lin, Qiang Shen, Penghui Lei, Xina Wang, and Ning Li. Microstructural Evolution of Dy_2O_3-TiO_2 Powder Mixtures during Ball Milling and Post-Milled Annealing // *Materials*. 2017, issue 10, p. 1-12.

53. G. Garcia-Martinez, L.G. Martinez-Gonzalez, J.I. Escalante-Garcıa, A.F. Fuentes. Phase evolution induced by mechanical milling in Ln_2O_3:TiO_2 mixtures (Ln=Gd and Dy) // *Powder Technology.* 2005, v. 152, issue 1-3, p. 72–78.

54. A.N. Guseva. *Methods of obtaining nanoscale materials. Course of lectures.* Ekaterinburg, 2007, 79 p.

55. A.V. Samokhin et al. Synthesis of nanosized zirconium dioxide powders and compositions based on it in thermal plasma of electric arc plasmatron // *Perspective Materials*. 2015, N 4.

56. A.V. Kushtym, N.I. Gonchar. Prospects for the use of jet-plasma processes for the manufacture of fuel and absorbing materials // *Collection of scientific articles "Nuclear Science and Energy through the Eyes of Youth: New Ideas, Research, Solutions"*. Odesa, Astroprint, 2011, p. 61-68.

57. N.V. Dedov et al. *Plasma chemical method for obtaining dysprosium titanate and/or dysprosium hafnate powder*: Patent RU 2686479, publ. 29.04.2019.

Робота виконана в рамках 2 етапу робіт за темою «Створення новітніх нейтронно-поглинаючих матеріалів для стрижнів системи управління і захисту з підвищеним ресурсом»(РН/13-2023), яка виконується в рамках програми «Горизонт 2020».

Article received 30.07.2024

СИНТЕЗ МАТЕРІАЛІВ НА ОСНОВІ СПОЛУК РІДКІСНОЗЕМЕЛЬНИХ ЕЛЕМЕНТІВ З ТИТАНОМ, ГАФНІЄМ ТА ЦИРКОНІЄМ ЯК ПЕРСПЕКТИВНИХ ПОГЛИНАЧІВ НЕЙТРОНІВ ЯДЕРНИХ РЕАКТОРІВ

І.О. Чернов, А.В. Куштим, С.В. Малихін

Представлено огляд методів синтезу титанатів, гафнатів і цирконатів рідкісноземельних елементів, у першу чергу диспрозію, що знайшли застосування в якості нейтронопоглинаючих матеріалів ядерних реакторів або є перспективними з причин їх високої радіаційної стійкості, фазової стабільності, сумісності з конструкційними матеріалами та корозійної стійкості. Наведено характеристики титанатів, гафнатів і цирконатів диспрозію, отриманих методами: високотемпературним твердофазним синтезом у компактованих сумішах вихідних оксидів; індукційним плавленням оксидів у «холодному» контейнері; хімічними методами, що ґрунтуються на сумісному осадженні та термообробці водних розчинів; механохімічною активацією порошків оксидів у планетарних млинах з подальшою термообробкою; плазмохімічним синтезом.